# Coherent anti-Stokes Raman spectroscopy of infrared multiphoton excited molecules

Shrenik Deliwala, Jay Goldman, Kuei-Hsien Chen,[a] Cheng-Zai Lü,[b] and Eric Mazur
*Department of Physics and Division of Applied Sciences, Harvard University, Cambridge, Massachusetts 02138*

(Received 15 June 1994; accepted 9 August 1994)

Time-resolved coherent anti-Stokes Raman spectroscopy is used to obtain the rovibrational energy distributions in polyatomic molecules following infrared multiphoton excitation. In addition to presenting new results on $SF_6$, we review previously obtained data on $SO_2$ and OCS. The data yield new details about infrared multiphoton excitation and intramolecular vibrational energy relaxation. In particular they show the significance of collisions in redistributing vibrational energy following excitation. The results also clearly show stronger intermode coupling and higher excitation in systems with increasing numbers of atoms per molecule.

## I. INTRODUCTION

Time-resolved measurement of vibrational spectra offers the exciting opportunity to monitor the evolution of vibrational distributions in highly excited molecules with many vibrational degrees of freedom. The vibrational distributions are obtained from the spectra by modeling each molecule as a system of coupled anharmonic oscillators.[1] This analysis yields a detailed picture of the excitation and subsequent flow of vibrational energy between oscillator modes, as well as intramode and collisional relaxation rates, and self- and cross-anharmonicities.

In the experiments described here, we excite a molecular ensemble using a pulsed $CO_2$-laser and probe the resulting vibrational distribution using time- and energy-resolved nonlinear Raman spectroscopy. The $CO_2$ laser is tuned to the ground-state frequency of an infrared active mode; it produces a broad distribution of excited vibrational modes via a process called infrared multiphoton excitation.[2–4] The highly excited ensemble is probed using multiplex coherent anti-Stokes Raman spectroscopy.[5,6] With this technique one obtains the complete rovibrational spectrum of the excited molecular ensemble in a single laser shot. A multiplex, single-shot measurement ensures that relative spectral intensities are reproducible, independent of shot-to-shot probe–laser energy fluctuations. Compared to spontaneous Raman or absorption spectroscopy, coherent Raman spectroscopy offers better noise rejection owing to directional separation of the signal from background scattered light and high spatial resolution. With nanosecond-pulse lasers and a sample at a pressure $\geqslant 1$ Torr, the coherent Raman signal is typically orders of magnitude larger than the spontaneous Raman or absorption signal.[6,7]

To determine the role of collisional energy redistribution we probed the molecules at various positions in a free jet expansion and compared these results to spectra obtained in a static cell. This allowed the study of energy relaxation in adiabatically cooled, nearly collision-free conditions, or alternatively at relatively high collision-rate, room-temperature conditions.

This paper presents newly obtained results on $SF_6$ and reviews previously published results on $SO_2$ and OCS. In $SO_2$ (Ref. 8) we observe direct $\nu_1$-mode excitation and distinguish between this process and excitation of the nearly resonant $\nu_2$-mode overtone. With OCS, direct overtone excitation is found,[9] and intra- and intermode energy transfer is time resolved in free jet samples.[10] The spectra of infrared excited $SO_2$ and OCS exhibit discrete spectra characteristic of low-level coherent excitation in small molecules with few vibrational modes. In contrast, $SF_6$ has a broad, nearly continuous spectrum, revealing $\nu_3$-mode pumping followed by rapid collisional energy redistribution to the nonpumped modes. Varying the collision rate in a molecular jet, we observe collision-rate dependent effects on the excitation and relaxation processes for all three molecules.

The paper is organized as follows. Section II presents a brief theoretical description of multiplex coherent anti-Stokes Raman spectroscopy and the infrared multiphoton excitation process in polyatomic molecules. Section III details the experimental apparatus and technique. In Sec. IV, we present the results for $SO_2$, OCS, and $SF_6$. These results illustrate how infrared multiphoton excitation and vibrational relaxation proceed in these systems, and what role collisions play in redistributing vibrational energy during and following excitation. They also demonstrate the utility of multiplex coherent anti-Stokes Raman spectroscopy for directly determining time-resolved excited state distributions.

## II. THEORY

### A. Multiplex coherent anti-Stokes Raman spectroscopy

Our goal is to time resolve an evolving rovibrational population distribution $N_{\{v,J\}}$, where $\{v,J\}$ labels a molecular rovibrational state ($v$ and $J$ are the vibrational and rotational quantum numbers, respectively). This population distribution $N_{\{v,J\}}$ is obtained from the spectrum of a Raman-active vibrational mode.

For infrared excitation of a polyatomic molecule well below the dissociation threshold, a normal mode description

[a]Current address: Institute for Atomic and Molecular Sciences, Academia Sinica, P.O. Box 23-166, Taipei, Taiwan.
[b]Current address: Massachusetts General Hospital, Boston, MA 02114

 0021-9606/94/101(10)/8517/12/$6.00  

is appropriate. As alluded to above, a polyatomic molecule is a good example of a system of coupled anharmonic oscillators. The normal mode frequency of each molecular vibration, $\omega_i$, is shifted by $\Delta\omega_i$ when the molecule is excited vibrationally into a state $\{v\}$. The shifts $\Delta\omega_i$ are given by[1]

$$\Delta\omega_i=\left(v_i+\frac{g_i}{2}\right)x_{ii}+\frac{1}{2}\sum_{\substack{j=1\\ i\neq j}}^{n}\left(v_i+\frac{g_i}{2}\right)\left(v_j+\frac{g_j}{2}\right)x_{ij}+\cdots, \tag{1}$$

where $v_i$ are the vibrational quantum numbers for each of the $n$ normal modes, $x_{ii}$ is a self-anharmonicity, $x_{ij}$ is a cross anharmonicity, and $g_i$ is the degeneracy of each mode. Note that for the molecules discussed here, both self- and cross anharmonicities are negative. The shifted frequency $\omega_i'$ of each rovibrational mode is then

$$\omega_i'=\omega_i+\Delta\omega_i+\frac{E(J)}{\hbar}, \tag{2}$$

where $E(J)$ is the energy of rotational state $J$. Inspection of Eq. (2) shows that the rovibrational spectrum of a probed mode can exhibit many peaks. Each peak will be shifted from the normal mode frequency by an amount proportional to the anharmonic coupling between the probed mode and an excited rovibrational mode.

Coherent anti-Stokes Raman scattering is a third-order nonlinear Raman process, in which two laser beams of frequency $\omega_1$ are mixed with a beam at $\omega_2$ to produce an output signal at $2\omega_1-\omega_2$. The frequency difference $\omega_1-\omega_2$ is chosen to be resonant with a single rovibrational transition $\omega_i'$.[6] *Multiplex* coherent anti-Stokes Raman spectroscopy (multiplex CARS[6]) incorporates a broadband $\omega_2$ beam with a spectral width that allows $\omega_1-\omega_2$ to cover the entire energy range of anharmonically shifted levels $\omega_i'$. In this way, the entire rovibrational spectrum containing all the $\omega_i'$ peaks is obtained in a single laser shot.

If intramode relaxation leads to equilibration among the vibrational levels of each molecular vibrational mode in the excited ensemble, then the vibrational distribution is characterized by a single temperature. The assumption of intramode equilibrium for the spectra analyzed here is justified because our time resolution (10 ns) is greater than the time scale for intramode equilibration.[11] The intensity of the multiplex CARS signal $I_{\mathrm{CARS}}$ is then proportional to

$$I_{\mathrm{CARS}}(2\omega_1-\omega_2)\propto\left|\sum_{\{v,J\}}\Delta N_{\{v,J\}}\frac{d\sigma}{d\Omega}\frac{1}{\omega_1-\omega_2-\omega_i'-i\Gamma}\right|^2\times I^2(\omega_1)I^2(\omega_2), \tag{3}$$

where $d\sigma/d\Omega$ is the Raman cross section of the mode, $\Gamma$ is the effective linewidth of the transition which in general is a function of vibrational excitation, and $\Delta N_{\{v,J\}}$ is the vibrational population difference between the lower and upper levels of the probed Raman-active transition, with $N_{\{v,J\}}$ given by

$$N_{\{v,J\}}=\frac{g_{\{v\}}\exp(-\Sigma\beta_v\hbar[\omega_i+\Delta\omega_i])g_{\{J\}}\exp(-\Sigma\beta_J E(J))}{\Sigma_{\{v,J\}}N_{\{v,J\}}}. \tag{4}$$

Here, $\beta_v=1/k_B\,T_{\mathrm{vibrational}}$ and $\beta_J=1/k_B\,T_{\mathrm{rotational}}$. The vibrational distribution, $N_{\{v,J\}}$, is obtained in practice by a numerical fitting procedure in which the vibrational and rotational temperatures $T_{\mathrm{vibrational}}$ and $T_{\mathrm{rotational}}$ are adjustable parameters, as discussed below.

When analyzing multiplex CARS spectra, one finds that the simplest experiment to interpret is one in which multiplex CARS probes one mode, while the $CO_2$ laser excites a different mode. This situation is easiest to interpret because peaks corresponding to self-anharmonicity terms are absent. In this case, assuming also that our multiplex CARS spectral resolution is narrower than the anharmonic shifts, the multiplex CARS ensemble spectrum appears as a sequence of discrete peaks as follows: (i) a molecular ground state peak (labeled a—cf. Fig. 2) at the probed mode normal frequency; (ii) a "primary" series of peaks (labeled b) downshifted from (a) by multiples of the cross anharmonicity between excited and probed modes; these peaks correspond to rovibrational excitation in the pumped mode; and (iii) a set of "satellite" peaks (c) downshifted from each of the primary peaks (a) and (b) corresponding to rovibrational excitation in non-laser-excited modes. In the more general case where the same mode is both excited and probed, a series of b and c peaks is observed multiple times [cf. Fig. 2(b)], once for each vibrationally excited level of the probed mode, with each sequence shifted in proportion to the self-anharmonicity of the probed mode.

In the experiments presented here, a simple discrete multiplex CARS spectrum is in fact realized for the experiments on OCS and $SO_2$. On the other hand, we find that multiplex CARS spectra of $SF_6$ can be either discrete or resemble a complex sequence of many overlapping peaks depending on collisional conditions, as discussed in Sec. IV.

### B. Infrared multiphoton excitation (IRMPE)

Intense laser beams are capable of exciting polyatomic molecules beyond the dissociation threshold, via a process known as infrared multiphoton excitation (IRMPE). This is true even though at low excitation intensities, vibrational excitation to highly excited states using a monochromatic pulsed laser is hindered by the anharmonic nature of each vibrational mode. In other words, if the pump laser wavelength is resonant with the ground state vibration of an infrared-active mode, each successive transition upwards in energy to higher vibrational levels is increasingly out of resonance with the pump laser.

Many models of infrared multiphoton excitation have been published.[4,12–15] Essentially, multiphoton excitation in polyatomic molecules by an intense infrared laser pulse proceeds through two distinct stages. Initially, the nearly resonant pulse excites the low-lying levels of the infrared-active mode, overcoming the relatively small anharmonicity of the vibrational levels via power broadening, collisional broaden-

ing, and rotational compensation. This stage of excitation is a coherent, stepwise process with the rate of each step proportional to the laser pulse intensity. At higher levels of excitation, the high density of states in all vibrational modes and increased intermode coupling to this dense manifold of levels leads to fast dephasing rates. The excitation then proceeds incoherently, proportional to pulse fluence. At the highest levels of excitation the process is no longer mode specific. This regime of level mixing and fast energy redistribution is often called the incoherent, or "quasicontinuum" regime.

To understand the details of infrared multiphoton excitation in a particular molecule, many parameters need to be determined. Of significant interest is whether a characteristic level of vibrational excitation can be identified at which a given molecule makes the transition from the coherent stage of excitation to the incoherent regime. While this transition may not be distinct in all systems, such information can be used in a given experiment to estimate the average number of laser quanta absorbed per molecule, or to predict properties of the relaxation process depending on pump-laser intensity. Also it is interesting to compare the onset of quasicontinuum excitation for different molecules. In general, larger polyatomic molecules have more vibrational modes and hence a relatively higher density of states at a given energy, leading to an earlier onset of incoherent excitation.[14,16,17] CARS spectra may indicate a transition to incoherent excitation when discrete spectra of a given excited molecule become broad or continuous at higher levels of excitation, corresponding to level mixing due to strong vibrational coupling. It is also important to be able to determine whether a transition to quasicontinuum excitation can ever be reached for a given system. Intense excitation resonant with a single rovibrational transition in the coherent regime can saturate the transition in the ensemble. If so, a rovibrational population "hole" will result which prevents further absorption of photons.[11,18,19] Multiphoton excitation will be inefficient in systems that cannot unsaturate or "fill" such a hole at a sufficient rate. One mechanism for hole filling is provided by collisions; collisions therefore enhance the infrared multiphoton excitation for some molecules.[18] Collisions when present are also an important mechanism for redistribution of excitation to nonpumped modes.[20] For these two reasons, collisions can play a significant role in infrared multiphoton excitation, possibly affecting the transition from the coherent to the incoherent excitation regime. Obtaining multiplex CARS spectra under variable collision-rate conditions allows us to test the role of collisions in the excitation process, and in the subsequent relaxation processes as well.

## III. EXPERIMENTAL APPARATUS

The experimental layout for the experiments discussed here is shown in Fig. 1. The infrared excitation source was a pulsed TEA $CO_2$ laser providing 200 ns pulses with a low intensity microsecond "tail." The pulses were truncated with a plasma shutter to produce pulses typically 40 ns in duration. The $CO_2$-laser beam was focused using a 0.15 m focal length cylindrical ZnSe lens to an elliptical cigar-shaped focus with 100 $\mu$m cross-sectional diameter centered over the smaller 80 $\mu$m CARS overlap region. Typical fluences were

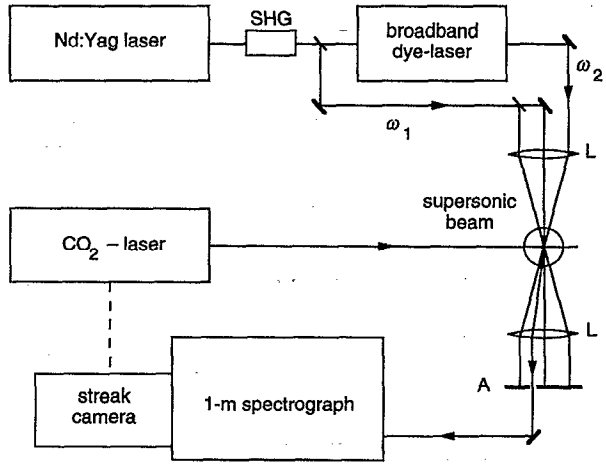


FIG. 1. Schematic layout of the apparatus for vibrational multiplex CARS spectroscopy. L: lens, A: aperture. The dotted line indicates an electronic trigger.

$\geqslant 3$ J/cm$^2$ at $\lambda = 10$ $\mu$m. Careful efforts were made to ensure that the multiplex CARS probe region was entirely enclosed within the infrared excited sample volume. The optical probe beams were generated by a Nd:YAG laser and custom-built dye-laser oscillator-amplifier setup. A Quantel YG471 frequency-doubled Nd:YAG laser produced linearly polarized, 300 mJ, 10 ns pulses at 532 nm. This green beam was split in three parts to produce two $\omega_1$ beams, and an $\omega_2$ beam with approximately 60 cm$^{-1}$ bandwidth. This broadband beam was generated in a prism-tuned dye-laser oscillator-amplifier, using Fluorescein 548 dye. As explained in Sec. II, the $\omega_2$ beam was tuned so that $\omega_1 - \omega_2$ covered the full spectrum of the rovibrational frequencies $\omega_i'$ of a given Raman-active mode.

To satisfy momentum conservation for the incident laser beams while at the same time achieving spatial separation of the probe and signal beams, we used a BOXCARS phase matching geometry.[6] The three incident beams were aligned parallel to each other, then focused into the sample chamber with a 0.3 m lens. The multiplex CARS signal was generated in the focal overlap region, which had an 80 $\mu$m beam waist. To align the detection optics, a HeNe laser beam was aligned parallel to the input beams through an appropriately placed pinhole so that the HeNe beam emerged at the phase matched angle collinear with the signal (CARS) beam. A second 0.3 m lens after the sample chamber recollimated all four beams. This geometry ensured a high rejection of background noise from the sample chamber windows and nonpumped portions of the gas sample, as well as rejection of scattered light from the probe beams. A 1 m spectrograph (Jarrell-Ash) was used to spectrally disperse the multiplex CARS signal. Following dispersion by the monochromator grating, the multiplex CARS signal was diverted out a side port of the monochromator instead of passing through an output slit. The entire spectrum was analyzed at once using Hamamatsu C1587 streak camera and vidicon video camera detector. The output was collected by a personal computer.

The effective spectral resolution of the apparatus was $\leq 0.1$ $cm^{-1}$.

In order to obtain time-resolved spectra, we varied the temporal delay $\tau$ between the excitation-laser ($CO_2$) and probe-laser pulses. To obtain spectra with $\leq 40$ ns time resolution, we desired synchronization of the lasers and streak camera to $\leq 1$ ns. For our commercial $CO_2$ laser, however, we typically observed a $\pm 30$ ns time jitter between the electrical trigger signal and the laser pulse output. We effectively eliminated this timing jitter from our measurement as follows. A custom-built fast pyroelectric detector and rf-amplifier circuit was used to optically trigger the streak camera from the $CO_2$-laser pulse. This triggering scheme provided $\leq 1$ ns timing jitter between the streak camera and the $CO_2$-laser pulse. We then took advantage of the unavoidable timing jitter between the YAG-laser pulse and the streak camera sweep, obtaining time-resolved spectra by collecting several hundred shots with random pump-probe delays $\tau$ over a $\pm 30$ ns interval and superposing them electronically in the streak camera. An advantage of collecting data in this way is that the entire time evolution of the spectrum can be obtained in a single streak camera video image which is then analyzed on a personal computer. This technique ensures precision referenced time delays, signal intensities, and spectral frequencies. Data analysis was performed on a personal computer using digital image-analysis software which extracted multiple narrow time-delay "slices" from each streak camera image. Each slice is a multiplex CARS spectrum for a given time delay $\tau$.

The gas samples were either static gas samples held at pressures from 1–100 Torr, or pulsed free jet samples. Our pulsed jet is a modified Toyota fuel injector nozzle with an output diameter $D=0.94$ mm. It is arranged in a vertical geometry and outputs gas pulses 1 ms in duration along the $z$ direction, synchronized with the laser pulses. The jet is mounted on a $xyz$ translation stage in a vacuum chamber maintained at $10^{-3}$ Torr by a roughing pump. Adjusting the translation stage allowed probing of the center of the molecular beam at various vertical distances $z$ downstream from the nozzle. The reservoir gas pressure behind the nozzle and the ratio $z/D$ were varied to obtain variable collision rates of ca. 10 collisions per 100 ns at $z/D=2$ to ca. 1 collision per 100 ns at $z/D=4$.[21–23] Rotationally and vibrationally cooled samples are obtained due to the adiabatic cooling which occurs in the free jet expansion. For $SF_6$, typical vibrational temperatures were 160 K at $z/D=2$ and 100 K at $z/D=4$, as determined from fits of the multiplex CARS ground state linewidths and from published data (for $SF_6$ at a reservoir pressure $p_{res} = 30$ psi, see Refs. 23 and 24). For smaller molecules cooling is more efficient;[25] for $N_2$, rotational temperatures as low as 10 K were obtained.

## IV. RESULTS AND DISCUSSION

### A. $SO_2$: Direct observation of $\nu_1$-mode excitation

Small polyatomic molecules like $SO_2$ are difficult to excite via infrared multiphoton excitation. Early studies of infrared multiphoton excitation in $SO_2$ were motivated by the discovery of inverse electronic excitation in this molecule.[26,27] In this process, excitation of electronic states occurs when highly excited vibrational states are populated via infrared pumping with intense 9 $\mu$m $CO_2$-laser lines. Our interest in this molecule arose because two possible pathways for the excitation are possible; excitation might proceed either via levels of the symmetric $\nu_1$ mode at 1151 $cm^{-1}$, or via even overtone transitions in the $\nu_2$ mode with 1035 $cm^{-1}$ steps. Because early investigations of infrared multiphoton excitation of $SO_2$ used the strong $9R(22)$ $CO_2$-laser line at 1080 $cm^{-1}$ which lies between $\nu_1$ and $2\nu_2$, it is not clear which modes play a role in the inverse electronic excitation. Recently, we showed that $\nu_1$-mode excitation is much more efficient, and is the dominant infrared multiphoton excitation pathway.[8] We also found that collisional enhancement of the infrared multiphoton excitation is critical for this molecule.

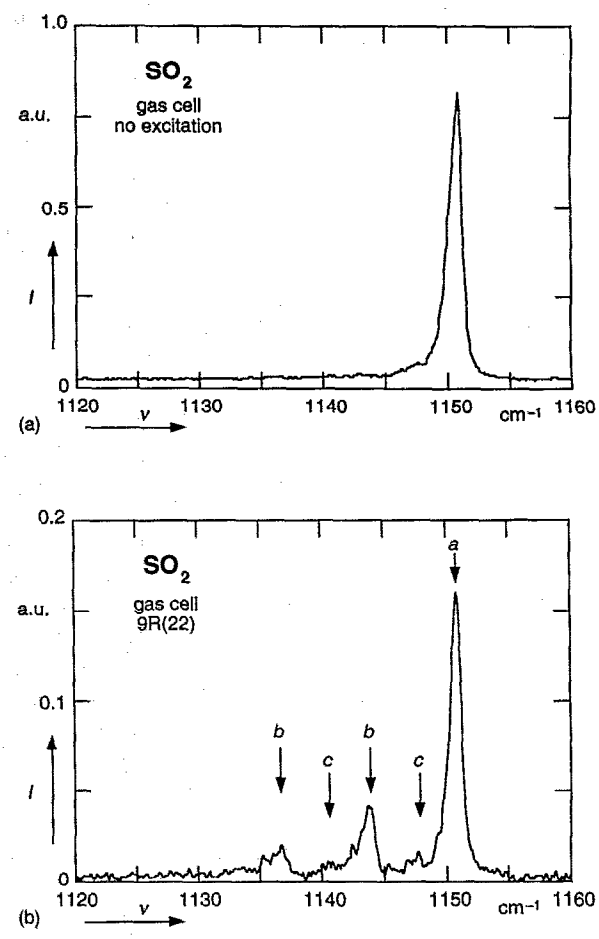


FIG. 2. Vibrational CARS spectra of $SO_2$ in gas cell samples at room temperature and 13 kPa (100 Torr). (a) Ground state (no excitation) spectrum. The large peak at 1151 $cm^{-1}$ corresponds to the $\nu_1$ mode. (b) An excited spectrum, 1.2 $\mu$s after 2 J/$cm^2$ excitation with $9R(22)$, showing excited states $b$ and $c$ (from Ref. 8).

We directly monitored the infrared multiphoton excitation in $SO_2$ by observing the intensity of the ground state CARS peak of $SO_2$ in gas cell and free jet samples following excitation with various $CO_2$-laser lines at fluences of about 2 J/$cm^2$.[8] Figure 2 shows the ground state and excited spectra

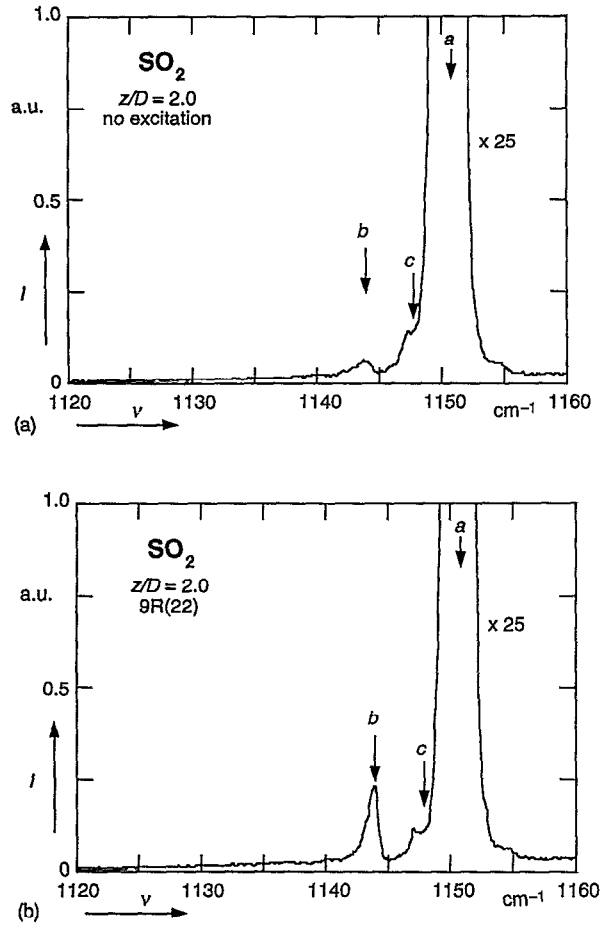


FIG. 3. Vibrational CARS spectra of $SO_2$ in a free jet (for $z/D=2.0$). Intensity scale is expanded to show small shifted peaks. (a) Ground state spectrum. (b) Excited spectrum, 200 ns after 1 J/cm$^2$ excitation with $9R(22)$. As a result of excitation, peak $b$ grows (from Ref. 8).

for $SO_2$ in a static gas cell. In these measurements, the intensity of the ground state peak at 1151 cm$^{-1}$ [labeled $a$ in Fig. 2(b)] decays rapidly following pumping by the $9R(22)$ laser line which is 71 cm$^{-1}$ detuned from the $\nu_1$ mode [cf. Figs. 2(a) and 2(b); note the change in vertical scale]. The decay of the ground state peak is accompanied by the appearance of two new peaks, labeled $b$. These peaks, shifted due to self anharmonicity of the $\nu_1$ mode, represent excitation of the $v=1$ and $v=2$ levels of the $\nu_1$ mode. The smaller peaks labeled c represent room temperature population of the $2\nu_2$ overtone mode and are not produced by the pump laser. No $2\nu_2$ overtone excitation is observed using any laser line, even for the $9P(32)$ line which is exactly resonant with $2\nu_2$.

Spectra obtained in free jet samples exhibit fewer and narrower spectral peaks, due to lower vibrational and rotational temperatures compared to gas cell samples. Figure 3(a) shows a spectrum obtained without excitation. The spectrum shows a very small amount of population in the $\nu_1$ mode (peak $b$) and the $2\nu_2$ overtone (peak $c$). Figure 3(b) shows the spectrum 200 ns after $9R(22)$ excitation. The increase in peak $b$ reflects the laser-excited population in the $\nu_1$ mode $v=1$ level. Again, no overtone excitation is observed. From these observations, it is clear that the excitation pathway must be via the levels of the $\nu_1$ mode.

Compared to the gas cell case, excitation in the free jet is less efficient overall, and even for comparable pump energies we do not observe excitation to the $v=2$ level of the $\nu_1$ mode. To discuss this decrease in excitation efficiency for free jet samples compared to gas cell measurements, we now recall our discussion in Sec. II. Two distinct possibilities need to be considered. One possibility is that lower collision rates in free jet samples lead to less collisional broadening and rotational hole filling, and hence lower excitation efficiency. It is possible therefore that these measurements illustrate rotational hole burning in this molecule. Another possibility is that the narrower rovibrational transitions characteristic of the adiabatically cooled free jet samples have poorer spectral overlap with the $CO_2$-laser lines used for excitation. This is likely, considering that the $9R(22)$ line is already significantly detuned (71 cm$^{-1}$) from the $\nu_1$-mode resonance at room temperature, and grows farther off resonance for a cooler distribution. The observed decrease of excitation efficiency in a free jet does not distinguish between these two possibilities, and most likely results from a combination of these effects. As we show in the next sections, our results with OCS and $SF_6$ exhibit similar characteristics.

Based on these results we can conclude that the laser intensities in this experiment are below the incoherent excitation regime for $SO_2$. This conclusion is supported by the lack of laser-induced excitation of any modes except for the laser-pumped mode, including the more highly excited gas-cell samples. This means that even in the case of gas-cell samples where collisions assist excitation, too few photons are absorbed per molecule to achieve strong coupling between laser-pumped and nonpumped molecular modes. As we show shortly, this is in marked contrast to the results for OCS and $SF_6$, where significant intra- and intermolecular population redistribution is evident.

### B. OCS: A nearly ideal coupled harmonic oscillator system

The linear OSC molecule has three widely separated vibrational modes which are weakly coupled owing to the small size of the molecule. Only the first overtone of the $\nu_2$ mode at 1054 cm$^{-1}$ can be resonantly pumped with 9 $\mu$m branch $CO_2$-laser lines in the 1041 to 1055 cm$^{-1}$ [$9P(24)$–$9P(10)$] range. Infrared multiphoton excitation of OCS with these laser lines is more efficient than $SO_2$. The Raman active symmetric stretch $\nu_1$ mode at 859 cm$^{-1}$ can be probed by multiplex CARS. Since this mode is not directly populated by the pump, and since it is only weakly coupled to the excited mode, this system is representative of the nearly ideal case discussed in Sec. II A. By pumping the overtone transition and probing the symmetric stretch, one can time-resolve intra- and intermolecular energy relaxation within the pumped mode and energy transfer to the nonpumped modes.

In gas-cell samples with pressures ranging from $10^3$ to $10^4$ Pa (10 to 100 Torr), the relatively high collision rate produces collisionally dominated dynamics.[9] Over the entire pressure range and pump–probe delay range ($\tau$=200 ns to 6

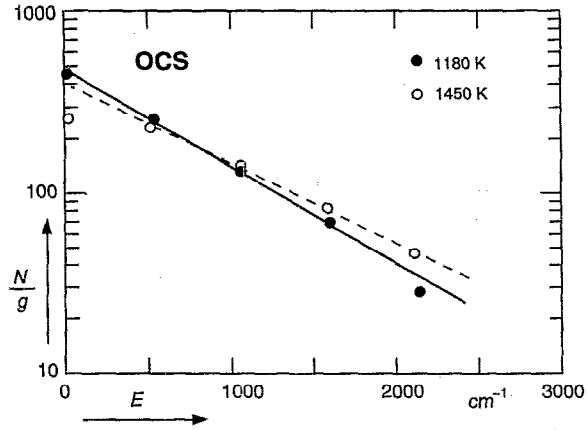


FIG. 4. Population distributions of the $\nu_2$ mode of OCS at $p=100$ Torr, 200 ns (closed circles) and 500 ns (open circles) after 9.2 J/cm$^2$ $CO_2$-laser excitation. The fits (solid and dashed lines) are Boltzmann distributions (from Ref. 9).

$\mu$s), nearly Boltzmann population distributions are observed in the $\nu_2$ mode (Fig. 4), even though only the overtone level is directly pumped. It is clear from these results that collisions redistribute the energy within the $\nu_2$ mode on a time scale shorter than the time resolution. This suggests that intermolecular processes dominate the observed dynamics of energy transfer.

Since the $\nu_2$-mode distribution is nearly Boltzmann, the temperature of this mode can be used as a parameter to study the excitation efficiency at various $CO_2$-laser lines. Table I lists the temperature of the $\nu_2$ mode after excitation with different $CO_2$ lines under otherwise identical conditions. As can be seen $CO_2$-laser lines with the smallest mismatch from a rovibrational transition in the $\nu_2$-overtone band produce the highest temperatures (1050 K). Laser lines with mismatches significantly greater than the power-broadened width of the infrared pulse (approximately 0.1 cm$^{-1}$) produce lower temperatures of 500–900 K. Thus we conclude that a major role of collisions in the excitation process itself is to enhance the pump laser overlap with available rovibrational transitions. A

TABLE I. Temperature of the OCS $\nu_2$ mode after excitation with different $CO_2$-laser lines at a fixed fluence of 7.6 J/cm$^2$, a pressure of 70 Torr, and a fixed pump–probe delay of 1 $\mu$s. The energy mismatch shown is between the laser wavelength and the closest rovibrational transition. The population of the initial rotational state, $N_J$, is also given (from Ref. 9).

| $CO_2$ laser line | Energy (cm$^{-1}$) | OCS transition (0,0,0)→(0,2$^0$,0) (cm$^{-1}$) | | $N_J$ | Mismatch (cm$^{-1}$) | $T_{\nu_2}$ (K) |
|---|---|---|---|---|---|---|
| $P(26)$ | 1041.28 | $P_{14}$ | 1041.48 | 0.85 | 0.20 | 750 |
| $P(24)$ | 1043.16 | $P_{10}$ | 1043.04 | 0.68 | 0.12 | 900 |
| $P(22)$ | 1045.02 | $P_5$ | 1045.03 | 0.38 | 0.01 | 1050 |
| $P(20)$ | 1046.85 | $P_1$ | 1046.64 | 0.11 | 0.21 | 500 |
| $P(18)$ | 1048.66 | $R_3$ | 1048.68 | 0.25 | 0.02 | 800 |
| $P(16)$ | 1050.44 | $R_7$ | 1050.33 | 0.51 | 0.11 | 500 |
| $P(14)$ | 1052.20 | $R_{11}$ | 1052.01 | 0.73 | 0.19 | 550 |
| $P(12)$ | 1053.92 | $R_{16}$ | 1054.13 | 0.92 | 0.21 | 450 |
| $P(10)$ | 1055.63 | $R_{20}$ | 1055.85 | 0.99 | 0.22 | 450 |

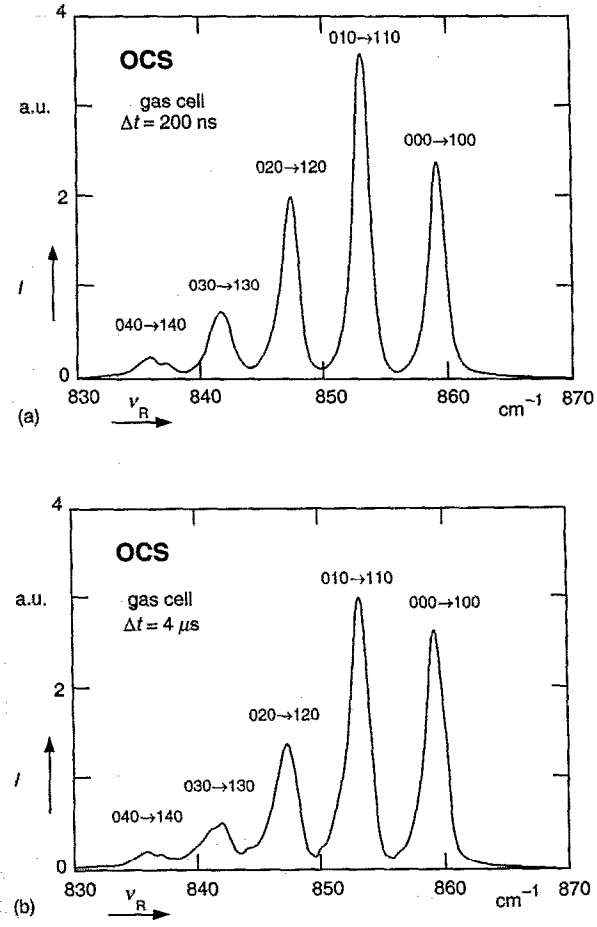


FIG. 5. Vibrational CARS spectra for excited gas cell OCS samples at room temperature and 13 kPa (100 Torr), with $9P(24)$ excitation at 9 J/cm$^2$ (a) 200 ns pump–probe delay. (b) 4 $\mu$s pump–probe delay. Note the formation of weak $\nu_3$-mode peaks (from Ref. 9).

second role of collisions becomes apparent in the time-resolved spectra. Figure 5 shows the OCS vibrational CARS spectrum shortly after $2\nu_2$ overtone excitation with the $9P(24)$ $CO_2$-laser line. Excitation of the first four levels of the $\nu_2$ mode is clearly visible. In Fig. 5(b), after a pump-probe delay of 4$\mu$s, we note the appearance of small CARS peaks corresponding to population in the $\nu_3$ mode (i.e., the unlabeled peaks between the identified transitions), as well as redistribution of vibrational population within the $\nu_1$ mode.

Experiments performed under low collision rates in a free jet support the conclusion that collisions dominate the energy redistribution dynamics.[10,28] We first performed a series of measurements to determine the excitation efficiency as a function of $z/D$ in the beam. This is achieved by measuring the population fraction excited out of the ground state at various $z/D$ at a fixed laser fluence and pump–probe delay. Figure 6 shows the excited state fractions obtained with the $9P(22)$ $CO_2$-laser line, which has the smallest energy mismatch for overtone pumping (see Table I). For values $z/D<3.8$ the excitation efficiency decreases as $z/D$ increases. For values $z/D>3.8$, the excitation efficiency re-

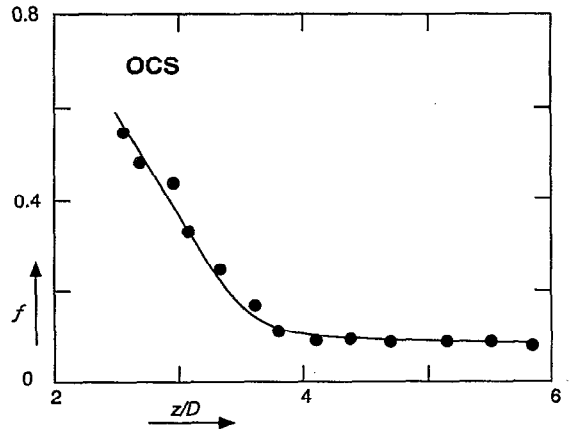


FIG. 6. The excited state fraction $f$ of ir-excited OCS in a free jet, as a function of increasing $z/D$ [$9P(22)$ excitation]. This fraction $f$ is a measure of the population excited out of the ground state. At $z/D>3.8$ the excitation remains constant, indicating that in this region collisions no longer contribute to excitation (from Ref. 9).

mains constant, indicating that under these conditions, collisions no longer play a significant role in the excitation process. We therefore investigated the CARS spectrum of OCS at short pump–probe delays for $z/D=3.8$. In these samples, only a single excited state peak [labeled 020→120 in Fig. 7(a)] appears in the spectrum at a 30 ns pump–probe delay. This peak corresponds to direct overtone pumping of the $2\nu_2$ level. For longer delays of 60 and 150 ns, a second peak [labeled 010→110 in Figs. 7(b) and 7(c)] appears and subsequently increases in intensity. This peak indicates transfer of energy into the $v=1$ level of the $\nu_2$ mode. Note also that on this time scale the population distribution in the $\nu_2$ mode is non-Boltzmann. These observations show that the infrared laser directly pumps the overtone transition, and suggest that collisions dominate the subsequent energy transfer to other levels of the $\nu_2$ mode and to the other modes.

A comparison of the OCS results obtained in gas cell and in free jet samples illustrates the effect of collisions in enhancing the infrared excitation and in the redistribution of vibrational energy after excitation to nonpumped modes. Only two $CO_2$-laser lines, each with a frequency mismatch less than the power broadened linewidth, produce detectable excitation in the jet. However, in the gas cell measurements, a high collision rate allows efficient pumping by $CO_2$-laser lines that are otherwise too far off resonance from a given rovibrational transition.

### C. $SF_6$: A two-ensemble picture

For a larger polyatomic molecule like $SF_6$, the density of states (and hence intermode coupling) increases rapidly as a function of increasing vibrational quantum number $v$. The

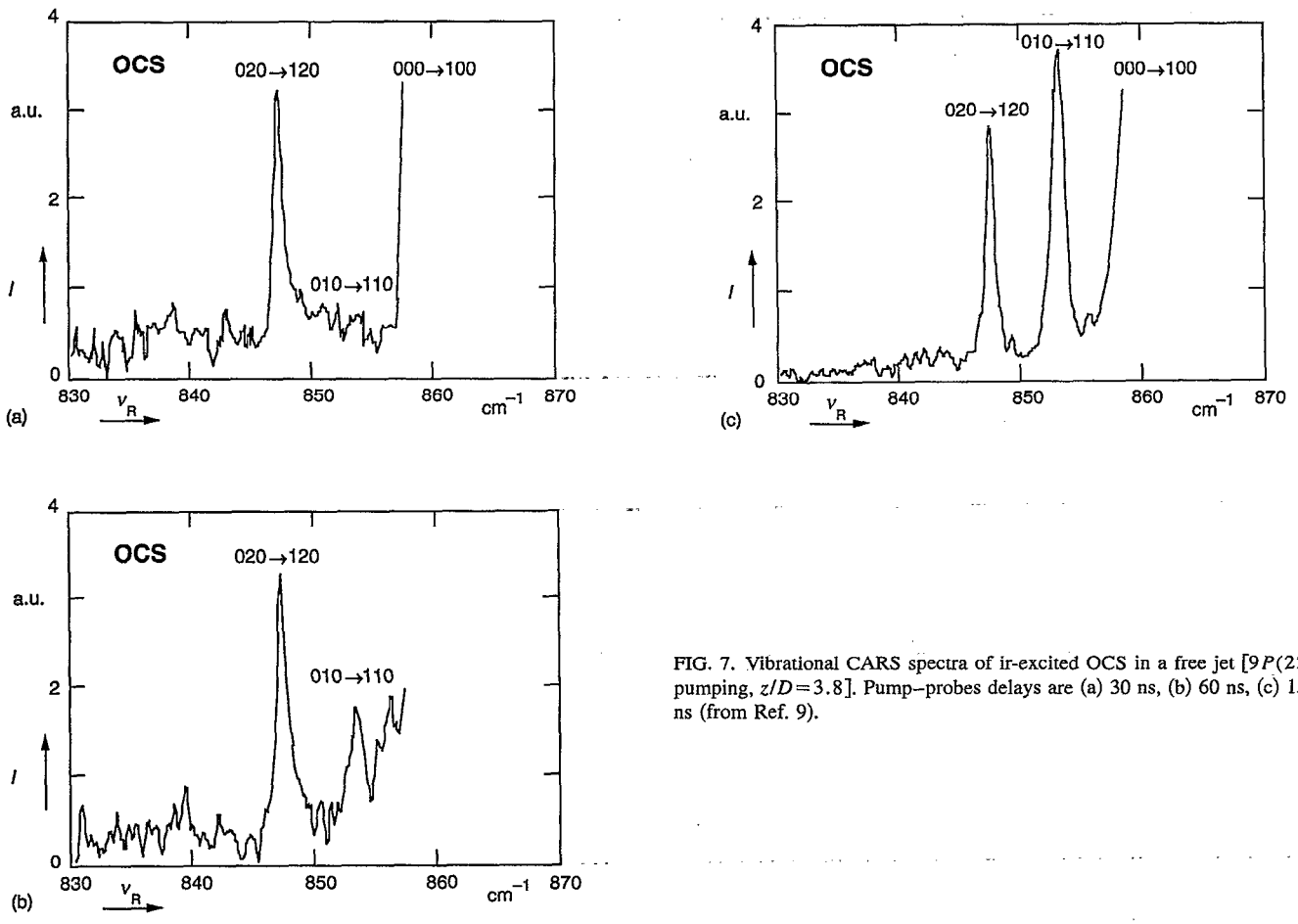


FIG. 7. Vibrational CARS spectra of ir-excited OCS in a free jet [$9P(22)$ pumping, $z/D=3.8$]. Pump–probes delays are (a) 30 ns, (b) 60 ns, (c) 150 ns (from Ref. 9).

resulting increase in excitation efficiency compared to the previous two molecules leads to high vibrational excitation in both the laser-excited and nonpumped modes. Since strong coupling between laser-excited and nonpumped modes produces efficient energy redistribution, multiplex CARS spectra of excited $SF_6$ tend to be complex and difficult to interpret compared to $SO_2$ or OCS spectra. Our results represent an effort to clarify contradicting reports in previously published work on $SF_6$. We find that collisional energy redistribution dominates the dynamics observed on a 100 ns time scale. We also report a new model for interpretation of the spectra. Analysis using these new results resolves contradictions in the literature and provides qualitatively simpler interpretation of the experiments described here and in the literature.

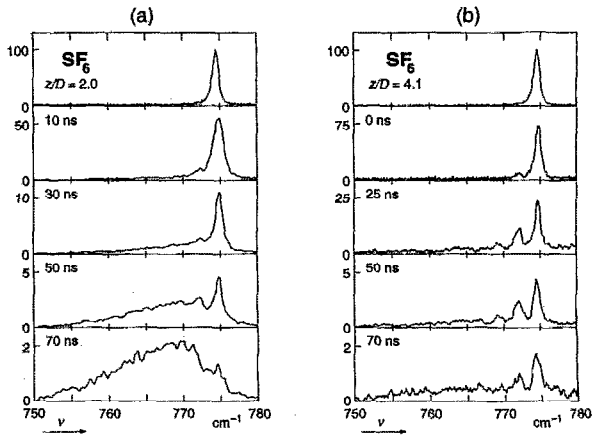


FIG. 8. Vibrational CARS spectra of ir-excited [$10P(20)$ line at 300 mJ/cm$^2$] $SF_6$ at various pump–probe delays for high and low collision rates. (a) High collision rate, 14 coll./100 ns. (b) Low collision rate, 1.4 coll./100 ns. Note change in vertical scale for different delays.

### 1. Previous work

Early studies of infrared multiphoton excitation in $SF_6$ were motivated by the discovery of efficient dissociation in samples pumped by a high-power $CO_2$ laser.[29–33] The molecule's similarity to $UF_6$ (Ref. 34) led to further research which produced applications in laser isotope separation. $SF_6$ has six normal modes; the $\nu_3$ mode is strongly infrared active and resonant with several 10 $\mu$m branch $CO_2$-laser lines.[35]

Coherent anti-Stokes Raman and other Raman probes have been used to investigate infrared multiphoton excitation in $SF_6$. The high efficiency of excitation produces markedly different results from those obtained for $SO_2$ and OCS. Using spontaneous Raman scattering, Bagratashvili *et al.* observed a dual spectral distribution of broad "hot" and "cold" ensembles created by $10P(20)$ excitation;[36] following excitation, the two ensembles appeared to dynamically equilibrate to a single distribution. Scanning-CARS gas-cell sample studies show selective low-energy $\nu_3$-mode excitation under low collision-rate conditions;[37] multimode excitation occurs at higher collision rates producing nearly continuous, more highly excited spectra.[38–40] These authors conclude that their results are supportive of the existence of an energy threshold marking the onset of excitation into "quasicontinuum" states. Furthermore the authors suggest that the nearly continuous spectral features at higher energies correspond to quasicontinuum states. These experiments place an estimate on the excitation threshold to quasicontinuum states at 6000 cm$^{-1}$, which is equivalent to an average absorption of about six $10P(20)$ photons per molecule.[38] On the other hand, a different series of CARS experiments with infrared excited $SF_6$ by Schweitzer *et al.*[41] yielded quite different results; while ground-state depletion was observed following $10P(20)$ pumping, no excited state peaks or broad continuous features as seen by the previous two groups were observed.

### 2. Results

The results of our measurements with variable collision rates in a jet explain the disparity between previous results, and show that, depending on excitation and collisional parameters, spectra consistent with the results of either group of researchers can be achieved. Furthermore, we find that collisions dominate the energy redistribution following laser excitation of the ensemble.

We performed multiplex CARS on the $SF_6$ symmetric $\nu_1$ mode at 775 cm$^{-1}$ while pumping the infrared-active $\nu_3$ mode with truncated 300 mJ/cm$^2$ $10P(20)$ $CO_2$-laser pulses in free jet samples.[28] By varying the collision rate and pump–probe delay, we obtained spectra that qualitatively reproduce both previous low and high collision rate measurements in which a continuum feature appears. Furthermore, the multiplex method yields accurate relative intensities of the evolving spectra at different collision rates or pump–probe delays. This allows quantitative modeling of the spectra, revealing (1) a "two-ensemble" population distribution produced via infrared multiphoton excitation, and (2) collision-rate-dependent energy transfer from the laser-pumped mode to the nonpumped modes after excitation.

Time-resolved spectra for both high and low collision rates are shown in Fig. 8. In both cases, one sees the intensity of the ground state at 775 cm$^{-1}$ decrease from the onset of infrared pumping (note change in vertical scale). Under high collision rates ($z/D=2.0$; 14 coll./100 ns), we observe rapid formation of a high-excitation broad spectral continuum within 50 ns [Fig. 8(a)]. At 70 ns delay, this continuum peaks at about 770 cm$^{-1}$, but then shifts towards higher excitation as time elapses. After several hundred nanoseconds (not shown in figure) the peak of the continuum reaches 750 cm$^{-1}$; this 25 cm$^{-1}$ shift corresponds to the absorption of about five infrared photons in the $\nu_3$ mode. The overall intensity of the continuum drops below detectable levels after about 500 ns. In contrast, results obtained at low collision rate ($z/D=4.1$; 1.4 coll./100 ns) exhibit selective $\nu_3$-mode excitation up to only the $v=3$ level, as shown by the individual peaks at a 50 ns delay in Fig. 8(b). A barely detectable broad continuum does arise at about 70 ns, with a peak around 765 cm$^{-1}$. The entire low-collision rate spectrum drops in intensity below detectable levels within 150 ns following excitation.

We also obtained an extensive set of data in which we examined the spectra at fixed pump–probe delays in the range 100 to 400 ns for *variable collision rates* (10–70 collisions/100 ns). In these data, the low collision-rate spectra exhibit discrete peaks as in Fig. 8(a), and the high collision-rate spectra exhibit the continuous features of Fig. 8(b). In fact, qualitatively similar spectral evolution is observed either as a function of the pump–probe delay (as in Fig. 8) or as a function of collision rate at fixed pump–probe delay.

### 3. Analysis

To extract the time-resolved population distribution $N_{\{v,J\}}$ we need to quantitatively model the multiplex CARS spectra. A spectral fitting procedure that computes the ensemble distribution for each of the six normal modes is not helpful for an intuitive interpretation; a six parameter model that assigns a vibrational temperature to each normal mode will not produce a unique fit. Instead we tested the assumption that the degrees of freedom might be reduced by computing the temperatures of only two Boltzmann ensembles, using one temperature for the laser-pumped mode and another temperature for the remaining nonpumped modes. This assumption essentially treats the nonpumped modes as a heat bath, similar to the description used in theoretical work by several authors.[2,4,17] The assumption of a heat bath is consistent with strong intermode coupling driven either by a high collision rate or fast intramolecular processes.

We wish to emphasize that multiplex CARS spectra require careful analysis for quantitative interpretation: when computing a spectrum with overlapping peaks, one needs to correctly add the real and imaginary parts of the line shapes of each peak [cf. denominator in Eq. (3)], as well as properly normalize each spectrum using the partition function. We performed this fitting procedure for the data shown in Fig. 8, but found that the spectral shape and intensity of the infrared excited spectra could not be fit using the aforementioned two-temperature model. One finds, for example, that a spectrum such as that obtained at 70 ns delay [Fig. 8(a)] cannot exhibit both a broad continuum *and* a small ground state peak in a two-temperature model.

Instead, we divided each of the two distributions, the pumped and nonpumped modes, into two hot and cold ensembles. Thus we have four parameters that describe the spectra: two temperatures (hot and cold) for the pumped mode and two temperatures for the nonpumped modes.[42] The motivation behind this model is the concept of a threshold in the multiplication excitation process, as discussed in Sec. II B. If a threshold exists, and the $CO_2$-laser fluence is near the threshold value, one would expect that some fraction of the laser-excited molecules will be excited above threshold. The multiplex CARS spectrum from the excited molecules will then be a convolution of signals from a highly excited above-threshold fraction (hot ensemble) and from a cooler below threshold fraction (cold ensemble).

Spectra from the four-temperature model are shown in Fig. 9 for the data of Fig. 8 using published values for the normal mode frequencies and anharmonic coupling constants of $SF_6$,[43,44] and adjusting the temperatures for optimal fit to the data. The resulting temperatures are constrained within $\pm 10\%$ for the fits shown in Fig. 9. Comparison of the two figures shows that the model produces curves that match *both* the spectral shape *and the relative intensities* of the spectra. Similar agreement was found for the data obtained as a function of collision rate. Table II summarizes the pumped-mode parameters for the calculated spectra in Fig. 9.

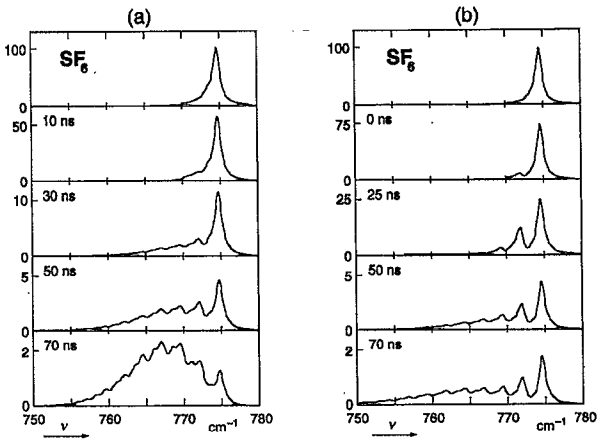


FIG. 9. Computed CARS spectra of $SF_6$ at various pump probe delays (a) 14 coll./100 ns (b) 1.4 coll./100 ns. See the text for explanation of computation algorithm. Temperature parameters obtained for these computed spectra are shown in Table II.

At high collision rates [Fig. 9(a)], the temperature of the $\nu_3$ mode hot ensemble increases from 900 K at a 10 ns delay to a high of 2500 K at 70 ns, with the hot ensemble containing 90% of the molecules. The $\nu_3$ mode cold ensemble peaks at 600 K. At low collision rates [Fig. 9(b)], the $\nu_3$ mode hot ensemble increases from 1000 K at a 25 ns delay to a high temperature of 3500 K at 70 ns, with the hot ensemble containing 80% of the molecules. The $\nu_3$ mode cold ensemble peaks at 800 K. The nonpumped, or heat bath, modes in both cases do not get as hot, nor is there much variation between the heat bath hot and cold ensembles. Typically the heat bath temperatures range from 300–500 K. The difference in peak temperatures reached in the high and low collision rate cases is attributed to a difference in $CO_2$-laser fluence.

As noted above, the spectral evolution observed as a function of pump–probe delay is qualitatively the same as the evolution observed as a function of collision rate at a

TABLE II. Parameters for the calculated spectra in Figs. 9(a) (14 coll./100 ns) and 9(b) (1.4 coll./100 ns). $\tau$ is the pump–probe delay. $T(\nu_3)$ shot and $T(\nu_3)$ cold refer to the $\nu_3$ mode hot and cold ensemble temperatures, respectively, with $F_{\text{hot}}$ equal to the fraction of the molecules in the hot ensemble.

| (a) 14 coll./100 ns | | | | (b) 1.4 coll./100 ns | | | |
|---|---|---|---|---|---|---|---|
| $\tau$ (ns) | $T(\nu_3)$ hot (K) | $T(\nu_3)$ cold (K) | $F_{\text{hot}}$ | $\tau$ (ns) | $T(\nu_3)$ hot (K) | $T(\nu_3)$ cold (K) | $F_{\text{hot}}$ |
| 10 | 900 | 350 | 0.30 | 0 | n/a | 500 | n/a |
| 30 | 1900 | 450 | 0.69 | 25 | 1000 | 740 | 0.70 |
| 50 | 2300 | 600 | 0.81 | 50 | 2500 | 780 | 0.71 |
| 70 | 2500 | 600 | 0.93 | 70 | 3500 | 800 | 0.81 |

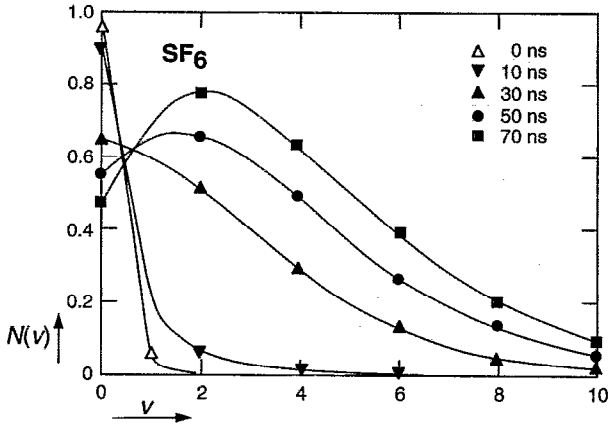


FIG. 10. Nonequilibrium vibrational population distributions $N(v)$ for the $\nu_3$ mode of $SF_6$ at various pump–probe delays for the high collision rate data in Fig. 8(a).

fixed pump–probe delay. As a function of collision rate at 160 ns pump–probe delay, the $\nu_3$-mode hot ensemble increases from 1200 K at 14 collisions/100 ns to 2000 K at 70 collisions/100 ns. The hot ensemble grows from 50% of the molecules to 80% in the same collision rate range. Similar to the data from the pump–probe delay experiment, the $\nu_3$ mode cold ensemble rises to 500 K while the heat bath temperatures range from 300–500 K.

The model curves of Fig. 9 directly yield the population distribution function $N_{\{v,J\}}$ [cf. Eq. (3)]. Vibrational population distributions for the $\nu_3$-mode data in Fig. 9(a) are shown in Fig. 10. These distributions are obtained by plotting the sum of the two Boltzmann distributions (the hot and cold ensembles) weighted by the computed fractions. The resulting nonequilibrium distributions show the evolution of the pumped mode population from its initial ground state condition to a highly excited state within 70 ns. Note that a single rotational temperature (70 K) is adequate to fit all the data included in Fig. 10; thus we have assumed no evolution of the rotational part of $N_{\{v,J\}}$ in producing the vibrational distributions.

From the distribution function $N_{\{v,J\}}$ we also determine the number of photons absorbed per molecule. As expected, we find that the number of photons absorbed is a constant for pump–probe delays greater than the laser pulsewidth. For the data obtained at a $CO_2$-laser fluence of 300 mJ/cm$^2$, the modeling yields a range of 3–5 photons absorbed per molecule. While the computed number of absorbed photons is constant within a few percent for a given data set it varies in the above range between different data sets. This is so even though we monitored the fluence from shot to shot and even though we took special care to ensure that the probed volume was uniformly pumped by the $CO_2$ laser, with no hot spots in the focal volume. The variability in the number of photons absorbed most likely arises from the 10% shot-to-shot intensity fluctuations in the $CO_2$-laser fluence. Because of the threshold in the excitation process, small fluctuations in the fluence lead to different ratios of hot-to-cold fractions. We note here that without quantitative modeling, these variations have gone unnoticed.

## 4. Discussion

Using a simple two-ensemble picture, we can successfully model the multiplex CARS spectra of laser-excited $SF_6$. We find that individual, resolved peaks in the spectra of less-excited molecules correspond to excited levels of the laser-pumped ($\nu_3$) mode, while the broad spectral continuum observed in more highly excited spectra corresponds to excited levels of the nonpumped modes. These nonpumped modes can essentially be treated as a single temperature heat bath. We also find that even for pump–probe delays much longer than the laser pulse excitation: (1) two ensembles persist, each with different heat bath and laser-excited-mode temperatures, and (2) the spectral evolution as a function of either pump–probe delay or collision rate is qualitatively the same.

These results imply that $SF_6$ does not reach intramode equilibrium within 100 ns of the infrared excitation in these experiments, and that this nonequilibrium condition can persist as long as 500 ns. Furthermore, the results show that collisional vibrational energy redistribution dominates all the dynamics observed.

A nonequilibrium distribution is observed when the multiphoton excitation produces two ensembles of excited molecules, one hotter than the other.[45] In each single molecule, intramolecular energy relaxation will redistribute vibrational energy within a few nanoseconds (assuming an average of 3–5 photons absorbed per molecule[11]). Thus an equilibrium distribution is rapidly reached within each ensemble of molecules. The multiplex CARS spectra show the convolution of these two overlapping ensembles, and the redistribution dynamics between them as they equilibrate to a single temperature. Because we observe these dynamics to be similar either as time progresses, or as the collision rate increases at a fixed time, we clearly see that these dynamics are dominated by intermolecular, or collisional, energy transfer.

The observed two-ensemble distribution supports the hypothesis that infrared multiphoton excitation can produce two distinct ensembles, as originally suggested by Letokhov.[17] The observation of (1) two distinct ensembles, and (2) high variation in the average number of photons absorbed per molecule, point to the existence of a threshold to incoherent excitation. For OCS and $SO_2$ the average number of photons absorbed per molecule is below the predicted threshold, but for $SF_6$, with an average of 3–5 infrared photons absorbed per molecule (3000–5000 cm$^{-1}$), we excite close to the predicted threshold (5000–6000 cm$^{-1}$).[16]

The broad continuum observed in the spectra consists of overlapping peaks of the nonpumped modes, populated predominantly by collisional energy transfer from the laser-pumped mode. This contrasts with the interpretation of Ref. 40, in which intramolecular redistribution is considered to be the dominant energy transfer mechanism in infrared multiphoton excitation of $SF_6$. Our interpretation furthermore shows that the broad highly excited feature in the $SF_6$ spectra does not, as previously stated,[38,40] correspond to "quasicon-

tinuum," or above-threshold, states directly populated by the laser. Instead, this broad feature is formed by rapid population of a heat bath of nonpumped modes via intermolecular energy transfer in collisions. Hence, collisions significantly enhance the overall excitation process.

In summary, we find that while the spectra of infrared excited $SF_6$ are more complex than the spectra of the smaller polyatomic molecules $SO_2$ or OCS, this system can nevertheless be simplified and quantitatively modeled within the context of the coupled anharmonic oscillator picture. The simplifications we use incorporate the concept of a threshold in the infrared multiphoton excitation. The resulting model fits to the data indicate that ir-excitation creates (1) a two-ensemble vibrational distribution and (2) a heat bath of nonpumped modes in molecules excited above threshold. These results are consistent with the experimental interpretation of Bagratashvilli *et al.*[46] in spontaneous Raman experiments, and with the theoretical work of Letokhov and others. The model yields dynamic population distributions $N_{\{v,J\}}$ and provides useful qualitative and quantitative insight into the excitation and energy redistribution process.

## V. CONCLUSION

In this paper we discuss multiplex CARS measurements of three different infrared multiphoton excited molecules. In each case, the measurements generate detailed qualitative and quantitative information about the vibrational population of an excited polyatomic, and the evolution of this population as inter- and intramolecular processes redistribute the energy. In $SO_2$ we observe direct $\nu_1$-mode excitation and distinguish between this process and excitation of the nearly resonant $\nu_2$-mode overtone. In OCS, direct overtone excitation is obtained and intra- and intermode energy transfer is time resolved. In $SF_6$, we directly observe $\nu_3$-mode excitation followed by collisional energy redistribution to a heat bath of nonpumped modes. Quantitative modeling of the $SF_6$ spectra resolves some long-standing inconsistencies between different published reports and supports the concept of a threshold for infrared multiphoton excitation. In the sequence of presentation ($SO_2$, OCS, $SF_6$) we see an increasing complexity in the infrared multiphoton excitation and the vibrational relaxation process as higher levels of excitation are produced in molecules with successively more vibrational modes.

## ACKNOWLEDGMENTS

The authors acknowledge helpful discussions with Professor N. Bloembergen and Professor M. J. Shultz. This work was funded by the Army Research Office, under Contract Numbers DAAL03-88-K-0114 and DAAL03-88-G-0078, by the Joint Services Electronics Program, under Contract Number N00014-89-J-1023, and by Hamamatsu Photonics K. K.

[1] G. Herzberg, *Infrared and Raman Spectra of Polyatomic Molecules* (Van Nostrand, New York, 1945), Vol. 2.
[2] N. Bloembergen and E. Yablonovitch, Phys. Today. **31**, 23 (1978).
[3] H. S. Kwok, E. Yablanowitch, and N. Bloembergen, Phys. Rev. A **23**, 3094 (1981).
[4] D. King, in *Dynamics of the Excited State,* edited by K. P. Lawley (Wiley, New York, 1982).
[5] M. D. Levenson and J. J. Song, in *Coherent Nonlinear Optics*, edited by M. S. Feld and V. S. Letokhov (Springer, Berlin, 1980).
[6] M. Levenson and S. Kano, *Introduction to Nonlinear Laser Spectroscopy* (Academic, San Diego, 1988).
[7] Y. R. Shen, *The Principles of Nonlinear Optics* (Wiley, New York, 1984).
[8] C.-Z. Lü, J. Goldman, S. Deliwala, K.-H. Chen and E. Mazur, Chem. Phys. Lett. **176**, 335 (1991).
[9] K. H. Chen, C. Z. Lü, L. A. Avilés, E. Mazur, N. Bloembergen, and M. J. Shultz, J. Chem. Phys. **91**, 1462 (1989).
[10] K.-H. Chen, thesis, Harvard University, 1989.
[11] R. C. Sharp, E. Yablonovitch, and N. Bloembergen, J. Chem. Phys. **74**, 5357 (1981).
[12] N. Bloembergen, I. Burak, and T. B. Simpson, J. Mol. Struct. **113**, 69 (1984).
[13] N. Bloembergen and A. Zewail, J. Phys. Chem. **88**, 5459 (1984).
[14] V. S. Letokhov, *Nonlinear Laser Chemistry* (Springer, Berlin, 1984), Vol. 22.
[15] D. P. Hodgkinson and A. J. Taylor, Mol. Phys. **52**, 1017 (1984).
[16] A. L. Malinovsky, E. A. Ryabov, and V. S. Letokhov, Chem. Phys. **139**, 229 (1989).
[17] A. Stuchebrukhov, S. Ionov, and V. Letokhov, J. Phys. Chem. **93**, 5357 (1989).
[18] W. Fuss and J. Hartmann, J. Chem. Phys. **70**, 5468 (1979).
[19] Y. A. Kuritsyn, G. N. Makarov, I. Pak, M. V. Sotnikov, I. I. Zasavitsky, and A. P. Shotov, in *Laser Chemistry*, edited by (Harwood Academic, City, 1988), Vol. 8.
[20] A nonpumped mode refers to a vibrational mode not in resonance with the pump laser frequency.
[21] P. Huber-Wälchli and J. Nibler, J. Chem. Phys. **76**, 273 (1982).
[22] D. Lubman, C. Rettner, and R. Zare, J. Phys. Chem. **86**, 1129 (1982).
[23] P. N. Bajaj and P. K, Chakraborti, Chem. Phys. **104**, 41 (1986).
[24] J. Anderson, AIAA J. **10**, 112 (1972).
[25] P. Huber-Wälchli, D. Guthals, and J. Nibler, Chem. Phys. Lett. **67**, 233 (1979).
[26] G. L. Wolk and R. E. Weston, J. Chem. Phys. **73**, 1649 (1980).
[27] T. B. Simpson and N. Bloembergen, Chem. Phys. Lett. **100**, 325 (1983).
[28] E. Mazur and C.-Z. Lü, in *Resonances*, edited by M. D. Levenson, E. Mazur, P. S. Pershan, and Y. R. Shen (World Scientific, Singapore, 1990).
[29] N. R. Isenor and M. C. Richardson, Appl. Phys. Lett. **18**, 224 (1971).
[30] T. F. Deutsch and S. R. J. Brueck, J. Chem. Phys. **70**, 2063 (1979).
[31] J. G. Black, P. Kolodner, M. J. Shultz, E. Yablanovitch, and N. Bloembergen, Phys. Rev. **19**, 704 (1979).
[32] J. Cahen-De Villardi, M. Clerc, P. Isnard, and J. M. Weulersse, J. Mol. Spectrosc. **84**, 319 (1980).
[33] U. Del Bello, W. Fuss, K. L. Kompa, and F. M. G. Tablas, J. Chem. Phys. **90**, 3055 (1989).
[34] A. Schultz and G. Marowsky, Appl. Phys. B **29**, 255 (1982).
[35] R. S. McDowell, H. W. Galbraith, B. J. Krohn, and C. D. Cantrell, Opt. Commun. **17**, 178 (1976).
[36] V. N. Bagratashvili, Y. G. Vainer, V. S. Doljikov, V. S. Letokhov, A. A. Makarov, L. P. Malyavkin, E. A. Ryabov, and E. G. Silkis, Opt. Lett. **6**, 148 (1981).
[37] S. S. Alimpiev, S. I. Valyanskii, S. M. Nikiforov, V. V. Smirnov, B. G. Sartakov, V. I. Fabelinskii, and A. L Shtarkov, JETP Lett. **35**, 361 (1982).
[38] R. V. Ambartsumyan, S. A. Akhmanov, S. M. Brodnikoshvskiĭ, S. M. Gladkov, A. V. Evseev, V. N. Zadkov, M. G. Karimov, N. I. Koroteev, and A. A. Puretskiĭ, JETP. Lett. **35**, 210 (1982).
[39] A. M. Prokhorov, in *Laser Spectroscopy VIII*, edited by W. Persson and S. Svanberg (Springer, Åre, Sweden, 1987).
[40] S. S. Alimpiev, A. A. Mokhnatyuk, S. M. Nikiforov, A. M. Prokhorov, B. G. Sartakov, V. V. Smirnov, and V. I. Fabelinskii, in *Laser Spectroscopy VIII*, edited by W. Persson and S. Svanberg (Springer, Åre, Sweden, 1987).
[41] E. L. Schweitzer and J. I. Steinfeld, Chem. Phys. **108**, 343 (1986).
[42] The heat bath hot and cold ensembles are found to vary within a narrow range (<100 K). Hence a further simplification might be made to a three-temperature model, i.e., a single temperature heat bath.

[43] A. Aboumajd, H. Berger, and R. Saint-loup, J. Mol. Spectrosc. **78**, 486 (1979).
[44] A. A. Puretzky and V. N. Zadkov, Appl. Phys. B **31**, 89 (1983).
[45] We note that spatially inhomogeneous laser pumping might lead to the production of two or more distinct ensembles. However, we ensured that the probed volume was well within the infrared-pump volume, ensuring a homogeneously pumped volume.
[46] V. N. Bagratashvili, V. S. Letokhov, A. A. Makarov, and E. A. Ryabov, *Multiple Photon Excitation Infrared Laser Photophysics and Photochemistry* (Harwood Academic, city, 1984).